Mechanisms underlying orientation selectivity of neurons in the primary visual cortex of the macaque

Hiromichi Sato*, Narumi Katsuyama, Hiroshi Tamura, Yoshio Hata and Tadaharu Tsumoto

Department of Neurophysiology, Biomedical Research Center, Osaka University Medical School, Suita, Osaka 565, Japan

1. Effects of blocking intracortical inhibition by microiontophoretic administration of bicuculline methiodide (BMI), a selective antagonist for $GABA_A$ receptors, on orientation selectivity of 109 neurones were studied in the primary visual cortex (V1) of anaesthetized and paralysed monkeys.

2. The averaged orientation tuning of visual responses of cells was poor in cytochrome oxidase-rich blobs of layer II/III and in layer IVcβ, moderate in layers IVb, IVcα and V, and sharp in the interblob region of layer II/III and in layers IVa and VI.

3. Iontophoretic administration of BMI reduced the sharpness of orientation tuning of cells to a varying extent in each layer. In most cells, furthermore, the originally ineffective stimuli induced visual responses during the BMI administration, suggesting that excitatory inputs evoked by the non-optimally oriented stimuli were masked by GABAergic inhibition. Nevertheless, the maximal facilitation was observed in the response to the optimally or near-optimally oriented stimuli.

4. There was a difference in such an effect of BMI among layers. Orientation selectivity of cells in interblobs in layer II/III and in layer IVb was sensitive to BMI whereas that of cells in layer VI was relatively insensitive to BMI, suggesting a larger contribution of excitatory mechanisms to the orientation selectivity in this layer.

5. In the orientation-selective cells, an analysis of the magnitude of excitation and inhibition evoked by stimuli at various orientations suggests that both inputs tune around the optimal orientation and their magnitudes are almost proportional to each other except at the optimal orientation. This analysis also indicates that the orientation tuning of inhibition had a less prominent peak around the optimal orientation than that of excitation. This dominance of excitation over inhibition around the optimal orientation may function to accentuate the response to the optimally oriented stimulus.

6. These results suggest that, in the monkey V1, the orientation selectivity of cells is largely dependent on the orientation-biased excitatory and inhibitory inputs which have a broader tuning profile, covering from the optimal to null-orientation, than that observed in extracellularly recorded responses at the control level.

Stimulus-specific response properties, such as orientation and direction selectivity, of neurones in the primary visual cortex (area 17) of cats and monkeys have been extensively studied since the pioneering work of Hubel & Wiesel (1962, 1968). In the original hypothesis of Hubel & Wiesel (1962), the orientation selectivity of cortical cells was explained by an alignment of receptive fields of geniculate afferents suitable for preferential responsiveness to particular stimulus orientation. In cats, several extracellular (Blakemore & Tobin, 1972; Bishop, Coombs & Henry, 1973; Sillito, 1975; Tsumoto, Eckart & Creutzfeldt, 1979; Sillito, Kemp, Milson & Berardi, 1980; Heggelund & Moors, 1983; Ramoa, Shadlen, Skottun & Freeman, 1986; Hata, Tsumoto, Sato, Hagihara & Tamura, 1988; Bonds, 1989) and intracellular (Ferster, 1986; Douglas, Martin & Whitteridge, 1988, 1991; Sato, Daw & Fox, 1991; Volgushev, Xing Pei, Vidyasagar & Creutzfeldt, 1993) studies were carried out to elucidate input mechanisms underlying the stimulus specificity.

* To whom correspondence should be addressed at Faculty of Health and Sport Sciences, Osaka University, Toyonaka, Osaka 560, Japan.

However, there seemed to be a discrepancy between the results of extracellular and intracellular studies.

The results of extracellular studies with microiontophoresis of bicuculline, a selective antagonist of γ-aminobutyric acid (GABA) receptors of the A type, suggested that there is a contribution of intracortical GABAergic inhibition to the stimulus specificity, even though there seemed to be variation in the degree of dependency on inhibitory inputs among cell types (Sillito, 1975; Tsumoto *et al.* 1979; Sillito *et al.* 1980). Using a cross-correlation technique, Hata *et al.* (1988) suggested that the inhibitory intracortical connection between cells with slightly different orientation preference contributes to the orientation selectivity of neurones in the primary visual cortex. These studies basically suggested that stimulus-specific inhibition arises primarily from cells with different orientation preference from that of the target cell.

On the other hand, intracellular studies (Ferster, 1986; Douglas *et al.* 1991; Sato *et al.* 1991) reported that inhibitory as well as excitatory inputs had a clear bias towards the optimally oriented stimulus. In these studies, however, the function of inhibitory postsynaptic potentials (IPSPs) evoked by the optimal stimulus on the orientation selectivity was not clear. Also, because of difficulties of intracellular recordings in *in vivo* preparations, the number of cells sampled in these studies was not large enough to assess the precise relationship between the orientation tuning profiles of excitatory and inhibitory mechanisms. With extracellular recordings, Chapman, Zahs & Stryker (1991) recently reported that in the ferret visual cortex, geniculo-cortical afferents are aligned to cover an elongated region of visual space mostly in line with the preferred orientation of cortical cells at the same location, which is consistent with Hubel & Wiesel's model. Thus, the question of whether GABAergic inhibition contributes to orientation selectivity still remains unresolved.

In primates, subcortical visual systems projecting to the primary visual cortex (V1) are segregated into at least two anatomically and physiologically distinct pathways called the parvocellular and magnocellular pathways (Livingstone & Hubel, 1988; Zeki & Shipp, 1988; Schiller, Logothesis & Charles, 1990; Merigan, Katz & Maunsell, 1991). These pathways give inputs to different layers of V1, i.e. parvocellular geniculate afferents to IV$c\beta$ and magnocellular afferents to IV$c\alpha$ (Blasdel & Lund, 1983). The inputs are further processed in a segregated way in the upper and lower layers. It is important to know the laminar difference of underlying mechanisms of the orientation selectivity in V1 to assess the functional organization of the cerebral cortex.

To our knowledge, there is no study which has addressed the question of the possible contribution of intracortical inhibition to the orientation selectivity of neurones in monkey V1 using bicuculline iontophoresis. In the present study, therefore, we examined effects of the blockade of intracortical inhibition by the iontophoretic administration of bicuculline methiodide (BMI) on orientation selectivity of monkey V1 neurones with particular reference to their laminar locations. Part of this study concerning the contribution of intracortical GABAergic inhibition to colour and direction selectivity of V1 cells has been reported elsewhere (Sato, Katsuyama, Tamura, Hata & Tsumoto, 1994, 1995).

METHODS

Preparation

Japanese monkeys, *Macaca fuscata*, weighing 3–6 kg (3–5 years old) were used in this study. Dexamethasone acetate (Decadron-A, Banyu Pharmaceuticals, Tokyo, Japan) was injected (0·1 mg, I.M.) 24–36 h before starting the experiment. Atropine (0·02 mg kg^{-1}, I.M.) and hydroxyzine hydrochloride (Atarax-Pfizer, New York, USA; 1 mg kg^{-1}, I.M.) were injected as premedication 20 min before starting surgery. Animals were anaesthetized with ketamine (5 mg kg^{-1}, I.M.) followed by a mixture of halothane (2–3%) or isoflurane (2–3%) and N_2O–O_2 (2:1), and the trachea and the femoral vein were cannulated. This level of gaseous anaesthesia was maintained until starting the recording experiment. Local anaesthetic, lidocaine, was given at pressure points and around surgical wounds. Monitoring of electric cardiogram (ECG) and heart rate was started following the initial anaesthesia. After the initial surgery, the animal was placed in a stereotaxic headholder, then paralysed with gallamine triethiodide (10 mg kg^{-1} h^{-1}, I.V.) or pancuronium bromide (0·08 mg kg^{-1} h^{-1}, I.V.) with a mixture of electrolytes, glucose (5%) and antibiotics (cefotiam dihydrochloride; Pansporin, Takeda, Osaka, Japan; 80 mg kg^{-1} day^{-1}), and maintained under artificial ventilation. Electrolyte solution in the infusion fluids was changed between Ringer solution (meq l^{-1}: 147 Na^+, 4 K^+, 4·5 Ca^{2+} and 155·5 Cl^-) and high-K^+ solution (meq l^{-1}: 35 Na^+, 20 K^+, 35 Cl^- and 20 L-lactate) every 3 h to adjust the electrolyte concentration in blood. Rate of infusion was 2 ml kg^{-1} h^{-1}.

The nictitating membrane was retracted and the pupil was dilated with topical application of a mixture of tropicamide (0·5%) and phenylephrine hydrochloride (0·5%) (Mydrin-P, Santen, Osaka, Japan). The eyes were refracted using O_2-permeable contact lenses so as to be focused on a tangent screen or CRT display at 57 cm in front of the animal. For the craniotomy, lidocaine was carefully injected subcutaneously over the skull before cutting the skin. A square-shaped hole (5 × 5 mm) was made by removing the skull and dura and arachnoid maters above the occipital cortex for penetration of recording electrodes under the anaesthesia mentioned above. The depth of anaesthesia during this period was judged as adequate since significant heart rate change (more than 10%) was not observed when the skin was cut.

During recordings of neuronal activity, the concentration of halothane or isoflurane was reduced to 0·3–0·5% or 0·5–1·0%, respectively, in N_2O–O_2 (2:1). Its concentration was increased if the heart rate changed by more than 10% by firmly pressing the facial skin of the animals with a small tip of ribbed forceps. The forceps stimulus could elicit quite strong and discernible pressure sensation for human subjects even though it was not painful. This test for the animal was repeated hourly. It is to be pointed out that usually we did not observe changes of the heart rate larger than 5%, suggesting that the anaesthesia was at an appropriate level.

Rectal temperature was maintained at 37–38 °C with a thermostatically controlled heating pad. End-tidal CO_2 concentration was adjusted to 3·5–4·0%. The ECG and heart rate were continuously monitored throughout the experiment. Blood pressure was monitored every 2 h with an automatic and non-invasive blood pressure monitor (ES-H51, Terumo, Tokyo, Japan) and its ranges were 87–127 mmHg (the systolic pressure) and 35–60 mmHg (the diastolic pressure). Throughout the course of experiments, which lasted 36–72 h, the monitored physiological parameters, the waveform of ECG, heart rate, range of blood pressure, end-tidal CO_2 concentration and body temperature, were kept stable. Volume of urination was monitored every 6 h and was ascertained to be almost equal to that of the infused electrolyte solution. Our procedures meet the regulations of the Animal Care Committee of Osaka University Medical School.

Visual stimulation

The positions and sizes of receptive fields of cells were first plotted on a tangent screen. Next, receptive field properties, dominant eye, optimal orientation and direction of stimulus, responsiveness to stationary flashed bar or spot, colour preference, and tuning to stimulus length and velocity were assessed with a hand-held Keeler Pantoscope. Then, visual stimuli produced by a computer (PC9801RA, NEC) were displayed on a CRT colour monitor (PC-TV455, NEC) using software originally written by Dr A. Mikami (Kyoto University, Japan) and modified by us for the precise and quantitative analysis of visual responses. Most of the experiments were done in a moderately light-adapted condition: luminance of visual stimuli and background were 19·7 and 1·4 cd m^{-2}, respectively. For a part of the experiments for the control of response saturation of cells during the BMI application, the luminance of the stimulus was changed between 19·5 and 1·6 cd m^{-2} against the background of 1·4 cd m^{-3}. For stimulation, a bar stimulus of preferred colour (red, yellow, green, blue or white) was moved across the receptive field, successively changing its orientation in 30 or 45 deg steps including the manually assessed optimal orientation.

Recording of single unit activity and iontophoresis

Recording sites were located at the postlunate gyrus 12·5–25 mm lateral to the mid-line and 30–40 mm posterior to the bregma. Triple-barrelled glass micropipettes were used for extracellular recordings of action potentials of single neurones in V1 and for iontophoretic administration of BMI and GABA to neurones under observation (Tsumoto, Masui & Sato, 1986). The tip of the recording pipette protruded by 15–20 μm from those of the drug pipettes. Tip diameter of each drug pipette was 2–4 μm. Drugs were dissolved in distilled water at the following concentrations and pH: BMI, 5 mM, pH 4·0; and GABA, 0·5 M, pH 4·0 (Sigma). The pH was adjusted with HCl and NaOH. The recording pipette was filled with 0·5 M sodium acetate containing 4% Pontamine Sky Blue for histological identification of recording sites. The electrode was angled from anterior to posterior 40–60 deg relative to the cortical surface in a parasagittal plane and with no obliquity in a coronal plane. Once activity of a single cell was isolated, its receptive field properties were assessed qualitatively with a hand-held Keeler Pantoscope and then peristimulus time histograms (PSTHs) of unit responses to visual stimulation were constructed with a signal processor (7T17, NEC-San-ei) before, during and after the iontophoretic administration of BMI. For visual stimulation, a bar of preferred colour and optimal length was moved across the receptive field and its orientation was successively changed in a clockwise manner in 30 or 45 deg steps; each stimulation trial consisted of twelve or eight differently directed stimulus motions. In this study, a stimulus oriented vertically and moved leftward was defined as orientation 0 deg. The direction of motion was always orthogonal to the orientation of the bar. Stimulus velocity was 3·2–7·2 deg s^{-1}. First, responses during six to twenty trials of stimulus presentation were accumulated to construct a control PSTH. Then, BMI was ejected from a drug pipette next to the recording pipette. Ejecting currents of BMI were between +2 and +60 nA, mostly between +5 and +40 nA. Retaining currents were between −5 and −20 nA. PSTHs during the BMI administration were constructed after the firing activity of the recorded cell reached a stable level, usually 2 or 3 min after starting the ejection. Intensities of the ejecting current of BMI were determined so that BMI antagonized the effects of GABA. GABA was iontophoresed from another drug pipette with an intensity of current necessary for complete suppression of visual responses of the first and every fifth cell in each penetration track. The ejecting currents of BMI were also adjusted so as not to elicit a marked increase in the spontaneous firing rate so as to prevent excessive activation which might lead to a saturation of spike firing. In the majority of cells, a few different intensities of ejecting current were applied to compare effects of different levels of cortical disinhibition. In most cases, orientation tuning curves during the BMI trials were made with data which showed the maximal reduction of the conventionally defined orientation selectivity index (cOSI) calculated with the following formula:

$$\text{cOSI} = 1 - (R_{\text{non-opt}}/R_{\text{opt}}),$$

where, R_{opt} represents the number of spikes in response to the forward and backward motion of an optimally oriented stimulus and $R_{\text{non-opt}}$ the number in response to a stimulus oriented orthogonal to the optimal. However, in cases where the increase of the BMI current did not elicit further increase of the optimal response, which is a possible sign of firing saturation, we took the data with a lower intensity of BMI. Three to ten minutes after stopping the BMI ejection, PSTHs of the recovery trials were constructed.

Histology

At the end of each penetration, dye marks were produced by passing tip-negative currents (intensity 7·5–10 μA; duration, 1 s at 0·5 Hz; 100 pulses). Dye deposits were placed at the stop point of each penetration and a few points with an interval of 500–1000 μm in the course of retracting the electrode. After the recording experiments, the animals were deeply anaesthetized with sodium pentobarbitone (40 mg kg^{-1}, I.V.) and perfused transcardially with buffered saline (pH 7·4) followed by 4% paraformaldehyde in 0·1 M phosphate-buffered saline (PBS). Blocks of occipital cortex were cut out and infiltrated with 30% sucrose in PBS for 48 h. Sixty-micrometre-thick frozen tangential or parasagittal sections of V1 were cut on a microtome and kept in PBS. Sections were histochemically stained for cytochrome oxidase (Wong-Riley, 1979). Then, the laminar location of recording sites and cytochrome oxidase-rich blobs in layer II/III were identified under microscopic observation. The system of Lund (1973) and Livingstone & Hubel (1984) was adopted for naming and classification of cortical layers. Shrinkage of cortical tissues was corrected by multiplying the ratio of measured dye mark distance to the value expected from the micrometer reading.

Expression of data

Unless otherwise stated, data are presented as means ± standard error of the mean (S.E.M.).

RESULTS

One hundred and nine cells whose laminar locations in area 17 of the cortex were histologically identified were analysed in the present study. All of them were tested with a moving bar stimulus which changed its orientation in 30 deg (for 82 cells) or 45 deg (for 27 cells) steps before, during and after the BMI application. Cells which did not show appropriate recovery (change in spike numbers was within ±30% of those of the control) from the BMI iontophoresis were omitted from analysis. Also, cells which were located at the border between layers were not included in the present study. Sampling of cells in this study was biased toward the superficial layers, particularly to cytochrome-rich blob cells in layer II/III, since this series of experiments was performed in parallel with another one aimed to study blob cells in layer II/III (Sato *et al.* 1994).

Laminar difference of orientation selectivity

More than half (58/109) of the cells were recorded from layer II/III. The remaining fifty-one cells were recorded from layers IV, V and VI. The orientation selectivity index (OSI) was calculated for each cell according to the following formula (Batschelet, 1965; Sáry, Vogels, Kovács & Orban, 1995):

$$\mathrm{OSI} = [(\sum R_i \sin(2O_i))^2 + (\sum [R_i \cos(2O_i))^2]^{0.5} / \sum R_i,$$

where, R_i represents the magnitude of response to each stimulus orientation, O_i. The rate of spontaneous activity, which was measured for 1 s before stimulus presentation, was subtracted from responses. The response to each stimulus orientation is expressed as a vector with direction $2O_i$ and length R_i. OSI is given by the normalized length of the vector sum of these vectors. This index takes a value between 1 and 0. An OSI value of 1 means complete selectivity to a particular orientation and no responsiveness to other orientations, while a value of 0 means equal responsiveness to any orientation.

Averaged OSIs of cells in each layer in control conditions (filled columns) and during BMI administration (shaded columns) are shown in Fig. 1. In control conditions, most cells in V1 were more or less sensitive to a particular stimulus orientation. The least orientation-selective layer was layer IVcβ (mean OSI = 0·07 ± 0·02), which is known to receive excitatory inputs from parvocellular geniculate afferents (Blasdel & Lund, 1983). Cells in the magnocellular recipient layer, IVcα, were also less selective to stimulus orientation than interblob cells in layer II/III and cells in layers IVa, IVb and VI. However, the mean OSI of layer IVcα cells, 0·27 ± 0·05, was significantly larger than that of layer IVcβ cells (Student's t test, $P < 0.01$). There was also a statistically significant difference (t test, $P < 0.0001$) in orientation selectivity between blob cells and interblob cells in layer II/III (mean OSI: 0·27 ± 0·04 and 0·54 ± 0·04, respectively). Cells in layers II/III (interblob region), IVa, IVb and VI were more orientation selective than the input layers (IVcα and IVcβ). Only three cells were recorded from layer V, and their orientation selectivity was too variable to draw a conclusion on the orientation selectivity of this layer.

In the following sections, effects of iontophoretically administered bicuculline methiodide (BMI) on the orientation selectivity of cells will be described in the order of layers in which they were located.

Layer II/III cells

Among the fifty-eight cells recorded from layer II/III, thirty cells were located in cytochrome oxidase-rich blobs and twenty-eight were in the interblob region. Generally, interblob cells had sharp orientation tuning whereas most blob cells showed a weak bias to a particular stimulus orientation, as reported previously (Livingstone & Hubel, 1984).

An example of records from an interblob cell is shown in Fig. 2. Peristimulus time histograms (PSTHs) of visual responses before, during and after the BMI administration and orientation tuning curves are shown. The PSTHs represent continuous recordings of firing responses to the stimulus sequentially changing its orientation in 30 deg

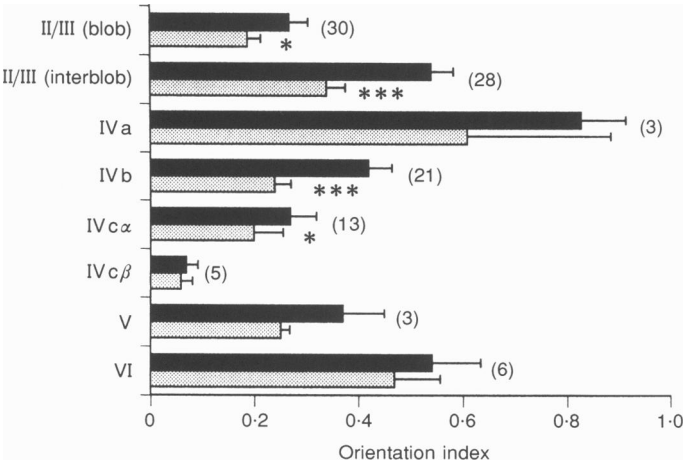

Figure 1. Averaged orientation selectivity index (OSI) of each cortical layer

Averaged OSI of neurones in each cortical layer in control trials (■) and BMI trials (▨). Horizontal bars indicate standard error of the mean; values of n are given in parentheses. Statistically significant decrease in OSI by the BMI administration is indicated by asterisks (* $P < 0.05$ and *** $P < 0.001$).
Mean ± S.E.M. OSIs in controls: cytochrome oxidase-rich blobs, 0·27 ± 0·04; interblobs, 0·54 ± 0·04; IVa, 0·83 ± 0·09; IVb, 0·42 ± 0·05; IVcα, 0·27 ± 0·05; IVcβ, 0·07 ± 0·02; V, 0·37 ± 0·08; and VI, 0·54 ± 0·09. Mean OSIs during the BMI administration: blobs, 0·19 ± 0·03; interblobs, 0·34 ± 0·04; IVa, 0·61 ± 0·28; IVb, 0·24 ± 0·03; IVcα, 0·20 ± 0·06; IVcβ, 0·06 ± 0·02; V, 0·25 ± 0·02; and VI, 0·47 ± 0·09.

steps, accumulated during ten trials of stimulus presentation (1 trial = presentation of twelve differently oriented/directed stimuli). This cell best and consistently responded to a moving bar stimulus, particularly of red colour, oriented at 150/−30 deg (the optimal orientation) and did not respond to stimuli oriented orthogonal to the optimal (Fig. 2*A a* and *A c*). The OSI of this cell during the control trials was 0·69. After starting the BMI administration with 20 nA of ejecting current for 2 min, the cell came to respond stably to any orientation of stimulus (Fig. 2*A b* and *B*, open circles) and the OSI decreased to 0·30. Since the tuning profile of responses during the blockade of $GABA_A$ receptor-mediated inhibition by BMI should reflect a tuning of excitatory inputs to this cell, the tuning curves during the BMI administration (Fig. 2*B*, open circles) imply that the excitatory input by itself has a bias toward the optimal orientation. On the other hand, the inhibitory mechanisms seem to operate for responses to any orientation of stimuli tested since the responses to all stimuli were facilitated during the BMI administration. These results suggest that there are broadly tuned excitatory inputs with a bias toward 150/−30 deg and that the GABAergic intracortical inhibition makes this cell orientation selective by suppression of firing activity of the cell.

On average, the interblob cells showed a statistically significant reduction of the averaged OSI from 0·54 ± 0·04 to 0·34 ± 0·04 ($P < 0·001$, *t* test) during the BMI administration.

Most blob neurones in layer II/III showed poor orientation selectivity except for cells located close to borders between blob and interblobs. Iontophoretically administered BMI facilitated firing activities of all the blob cells recorded. An example of effects of BMI on the orientation tuning of a blob cell is shown in Fig. 3. This cell responded to stimuli of all the orientations with a weak bias towards −120 deg in the control trials (Fig. 3*A a*, *A c* and *B*). The OSI of this cell during the control trials was 0·14. During the BMI administration with 30 nA, responses to all stimuli were facilitated (Fig. 3*A b* and *B*, open circles) and the OSI increased slightly to 0·18. On average, however, the blockade of intracortical inhibition induced a statistically significant reduction of OSI ($P < 0·05$, *t* test) in the blob cells from 0·27 ± 0·04 to 0·19 ± 0·03. These results suggest that the intracortical inhibition operates even in the poorly oriented blob cells for any stimulus orientation. However, the bias of excitatory inputs towards a particular orientation was not strong enough to make the responses orientation selective.

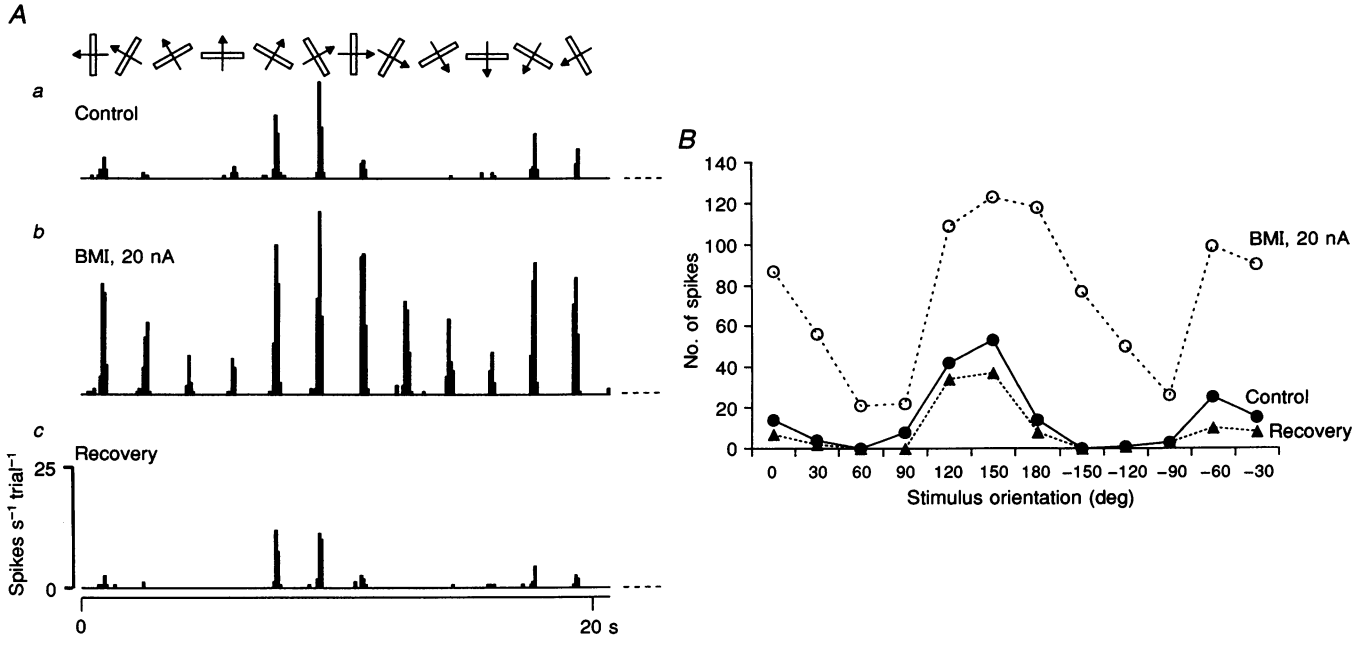

Figure 2. An example of the effect of BMI on visual responses of a layer III interblob cell

A, peristimulus time histograms (PSTHs) of responses to visual stimuli before (*a*), during (*b*) and after (*c*) iontophoretic administration of BMI with a current of 20 nA. A light bar (1·23 × 0·33 deg) was moved across the receptive field with a velocity of 4·0 deg s^{-1}. As shown at the top, stimulus orientation and direction were successively changed in a clockwise manner with 30 deg steps from 0 deg (vertical orientation and leftward movement). Ten sweeps at each orientation. Bin width, 80 ms. The recovery PSTHs were obtained 2–6 min after cessation of BMI administration. Dashed line at the right of each PSTH indicates spontaneous discharge level. *B*, orientation tuning curves of responses shown in *A*. Number of spikes in responses is plotted against stimulus orientation.

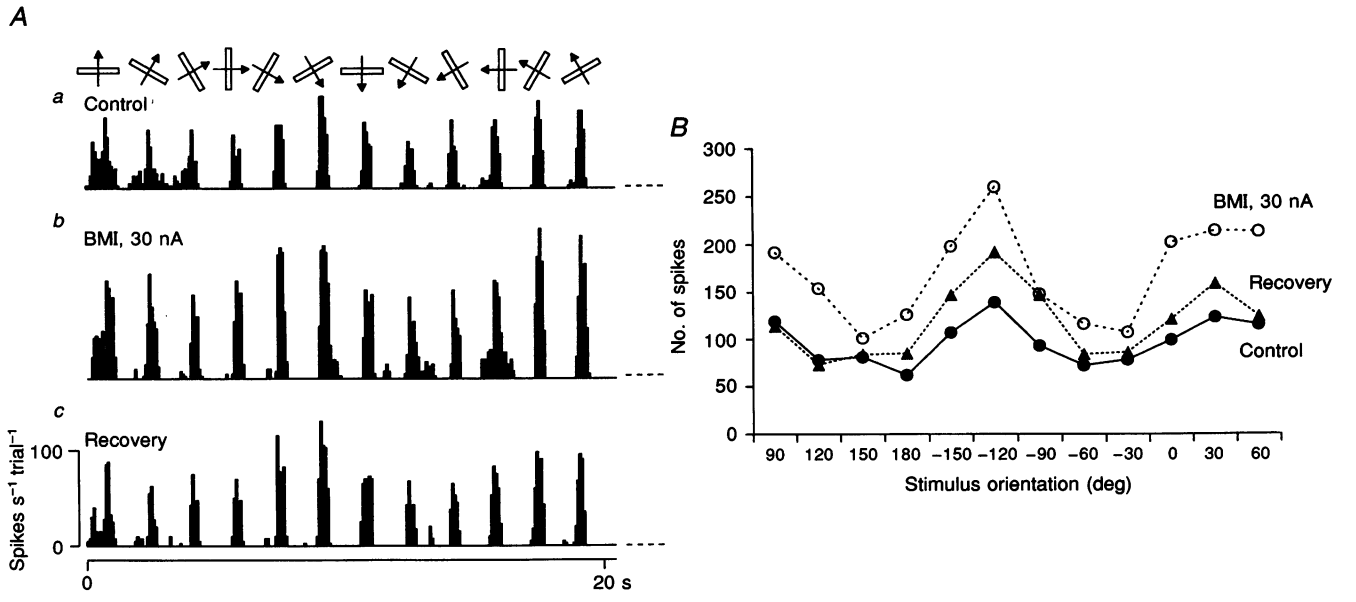

Figure 3. An example of the effect of BMI on visual responses of a layer III blob cell

A, PSTHs before (*a*), during (*b*) and after (*c*) iontophoretic administration of BMI. Seven sweeps for each stimulus orientation. Size and velocity of stimulus bar were 1·64 × 0·41 deg and 4·0 deg s^{-1}, respectively. Bin width, 80 ms. The recovery PSTHs were obtained 4–7 min after stopping the BMI administration. Other conventions, as in Fig. 2. *B*, orientation tuning curves of responses shown in *A*.

Distribution of OSI of cells in layer II/III during the control and BMI administration is shown in Fig. 4. In the control (abscissae), the distributions of OSI of blob cells (Fig. 4*A*) and of interblob cells (Fig. 4*B*), were clearly different from each other. The OSIs of blob cells had a distribution with a mode in the range of 0–0·2, indicating that the orientation selectivity of blob cells is essentially poor. On the other hand, those of the interblob cells had a broad distribution with a mode in the range of 0·5–0·7. During BMI administration (ordinate), the distribution of OSIs of both groups shifted to smaller values and fell below the diagonal line in each graph. During the blockade of the intracortical inhibition, the distribution of OSIs of the interblob cells mostly took a range of less than 0·6, which is comparable to that of the blob cells during the BMI administration, with a slight bias toward the larger values. This suggests that intracortical inhibition can more effectively enhance the orientation selectivity of those interblob cells that receive excitatory inputs that are better tuned than those of blob cells. This inhibitory mechanism makes the difference between blob and interblob cells in the orientation selectivity of spike responses more distinct than those responses at the input level.

Layers IVa and IVb

Cells recorded from both layers IVa and IVb had quite similar response properties in terms of orientation and direction selectivities. Since layer IVa is very thin, only

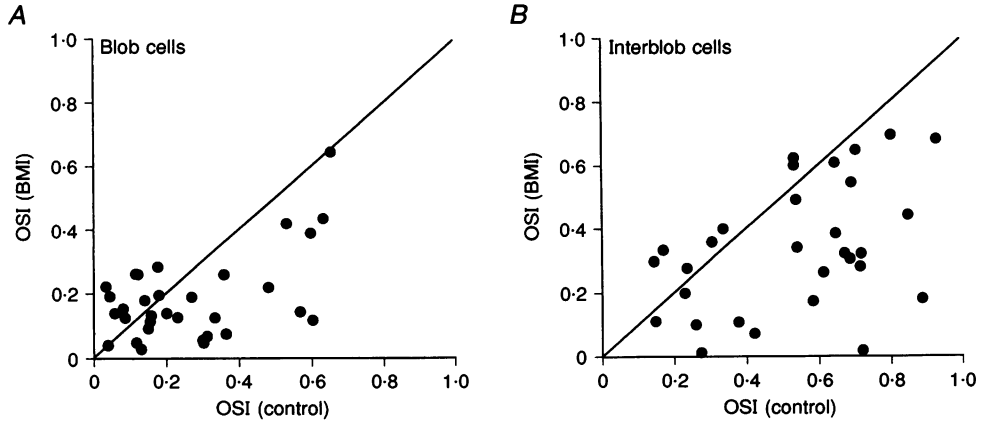

Figure 4. Scatter plots of OSI of layer II/III cells during the control and BMI administration

Abscissae, OSI at the control and ordinate, OSI during the BMI administration. *A*, blob cells, $n = 30$. *B*, interblob cells, $n = 28$.

three cells, which were confirmed to be located within this layer, were included in the present analysis. In the control, all the three layer IVa cells were strongly orientation selective (Fig. 1). Two of the three cells were also strongly direction selective, i.e. they had a marked preference for one direction of stimulus movement at the optimal orientation. During BMI administration, the mean OSI of the layer IVa neurones decreased from 0·83 ± 0·09 to 0·61 ± 0·28 (Fig. 1), although this change was statistically insignificant ($P > 0·05$). However, the sample size of layer IVa cells is too small to draw a conclusion about the underlying mechanism of orientation selectivity in this layer. Most of the twenty-one cells recorded from layer IVb also had well-oriented and uni-directional visual responses (Figs 1 and 5*A*). The iontophoretic administration of BMI facilitated firing of cells in this layer and averaged OSIs of the twenty-one layer IVb neurones decreased from 0·42 ± 0·05 to 0·24 ± 0·03 (Fig. 1). The difference between these two values was statistically significant ($P < 0·001$, t test). The change in OSI of individual cells in layer IVb (Fig. 5*A*) was similar to that in layer II/III interblobs (Fig. 4*B*); the major population of cells of layer IVb (18/21) reduced its OSIs during the BMI administration.

Layers IVcα and IVcβ

Thirteen and five cells were recorded from layers IVcα and IVcβ, respectively. Most of the cells in these layers had a moderate or weak orientation preference. However, there is a significant difference in the distribution of OSIs between these two layers, i.e. OSIs of the majority of layer IVcα cells were larger than 0·2, whereas those of all the IVcβ cells were less than 0·2 (Fig. 5*B* and *C*). In fact, a certain population of layer IVcα cells had clear orientation selectivity, as reported previously (Blasdel & Fitzpatrick, 1984; Livingstone & Hubel, 1984). An example of a IVcα cell is shown in Fig. 6. This cell responded best to stimuli oriented 90/−90 deg with a directional bias to −90 deg (Fig. 6*A a*, *A c* and *B*, filled circles and triangles). BMI administration with 10 nA increased the firing activity of this cell and facilitated responses to all stimuli fairly evenly (Fig. 6*A b*), suggesting an operation of poorly oriented inhibitory inputs to this cell. Consequently, the OSI of this cell slightly reduced from 0·26 (at the control) to 0·15 (during the BMI administration). However, a bias of response toward the original optimal orientation remained during the BMI administration (Fig. 6*B*, open circles), suggesting the presence of orientation-biased excitatory inputs to this layer IVcα cell.

Only five cells were recorded from layer IVcβ and none of them showed sharp tuning to a particular stimulus orientation. During the BMI administration, responses which originally had poor tuning to stimulus orientation were generally facilitated without bias to particular orientations, suggesting a presence of orientation-insensitive excitatory and inhibitory inputs to neurones in this layer.

In these layers, the blockade of intracortical inhibition by BMI facilitated visual responsiveness in all the cells tested

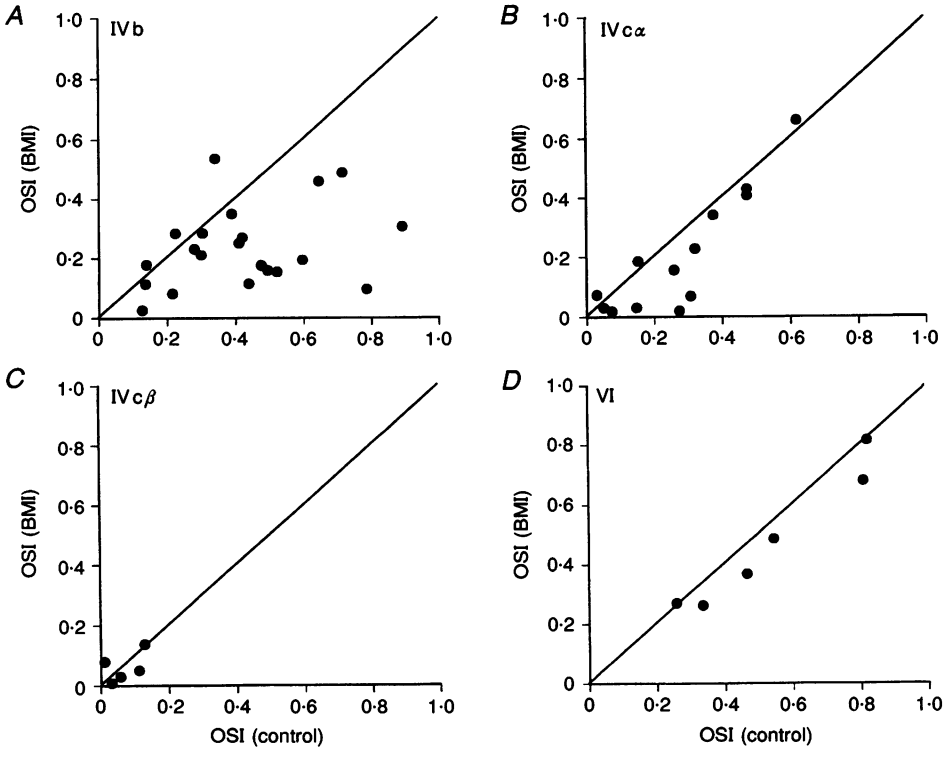

Figure 5. Scatter plots of OSIs of cells recorded from layers IVb, IVcα, IVcβ and VI

A, layer IVb, $n = 21$; *B*, layer IVcα, $n = 13$; *C*, layer IVcβ, $n = 5$; *D*, layer VI, $n = 6$. This analysis was not done for layers IVa and V since the sample size of these layers was too small ($n = 3$, in both layers).

and averaged OSIs nominally decreased from 0·27 to 0·20 for layer IVcα neurones and from 0·07 to 0·06 for layer IVcβ neurones (Fig. 1). The change was statistically significant for layer IVcβ ($P < 0·05$, t test) but not for IVcα ($P > 0·05$). The overall change in tuning was similar among layer IVc cells and blob cells in layer II/III.

Layers V and VI

Three layer V and six layer VI cells were analysed in the present study. The layer V cells, on average, had moderate tuning for stimulus orientation in the control (OSI = 0·37 ± 0·08, $n = 3$; Fig. 1). During the BMI administration, the mean value of OSI decreased to 0·25 ± 0·02 (Fig. 1), but this change was statistically insignificant ($P > 0·05$, t test). However, the number of recorded cells was too small to make a conclusive statement. The layer VI cells showed fairly sharp orientation tuning on average (OSI = 0·54 ± 0·09, $n = 6$) and their orientation tuning was resistant to the effect of BMI (Figs 1 and 5*D*). An example of records from a layer VI cell is shown in Fig. 7. This cell had well-oriented (0/180 deg) and bidirectional responses in the control trials (Fig. 7*A a* and *B*). It did not respond to stimuli at the orientation perpendicular to the optimal (null orientation) and its OSI during control responses was 0·82. An iontophoresis of BMI with ejecting current of 20 and 40 nA strongly facilitated responses to the preferred orientation and only weakly facilitated those to the non-preferred orientations (Fig. 7*A b*, *A c* and *B*). The maximal facilitation took place in response to the optimally oriented stimuli and sharpness of orientation tuning remained during the blockade of cortical inhibition (OSI = 0·81 and 0·65 with 20 and 40 nA of BMI, respectively; Fig. 7*B*) even though small responses emerged during the BMI administration with 40 nA. The mean OSI of the six layer VI cells was not significantly decreased during the BMI administration ($P > 0·05$, t test; Figs 1 and 5*D*). These results suggest that the orientation tuning of cells in this layer is largely dependent on orientationally tuned excitatory inputs even though the intracortical inhibition makes the tuning width slightly narrower.

Input mechanism of orientation-selective cells

To elucidate laminar characteristics of input mechanisms underlying the orientation selectivity, we drew averaged orientation tuning curves of cells in each layer of V1 (Fig. 8). Twenty-six strongly orientation-selective (OSI ⩾ 0·50) cells, which were recorded from layers II/III (interblobs), IVa, IVb and VI and tested with a stimulus changing its orientation in 30 deg steps, were chosen for this analysis. Cells recorded from layers IVcα, IVcβ and V, and blobs in layer II/III were omitted from this analysis because of their poor or variable orientation tuning. In Fig. 8, response sizes during the control and BMI trials of individual cells were normalized to the response to the optimal orientation during the BMI administration and then averaged. In the control (continuous line), the tuning width for the layers did not markedly differ from one another, and half-widths at half-height of the tuning peak for layers II/III (interblob),

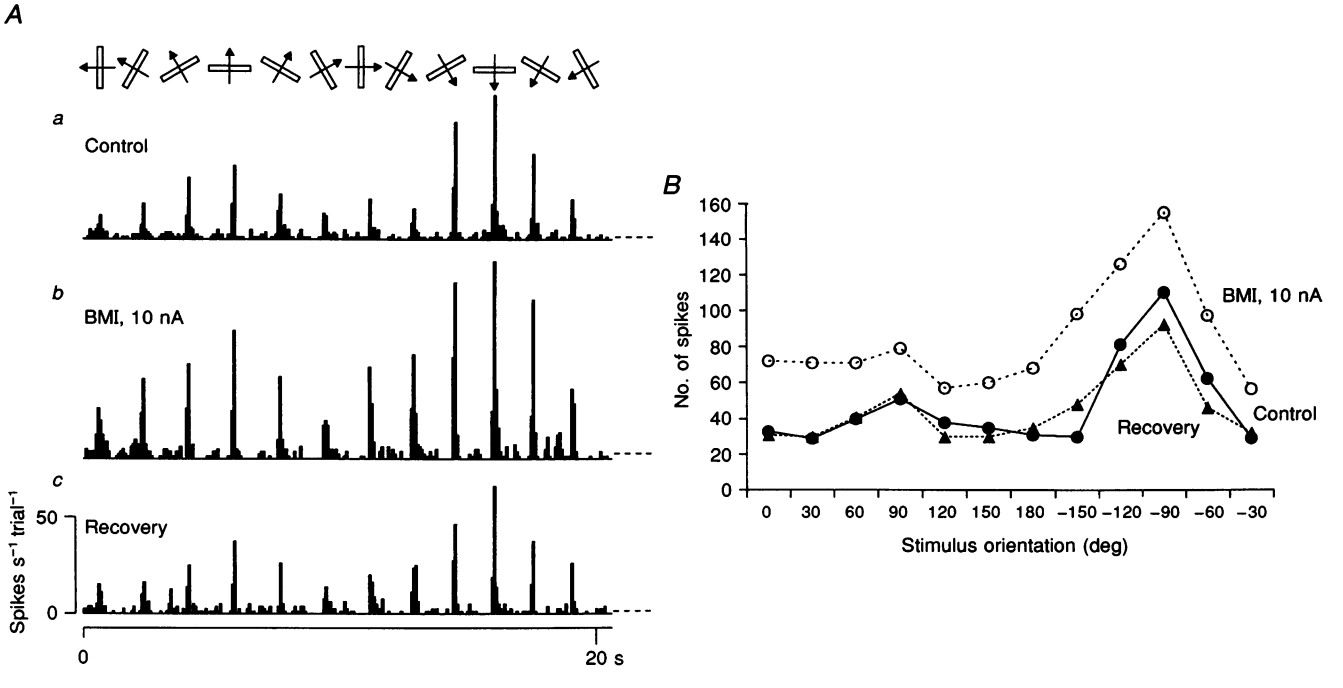

Figure 6. An example of the effect of BMI on visual responses of a layer IVcα cell

A, PSTHs before (*a*), during (*b*) and after (*c*) iontophoretic administration of BMI. Ten sweeps for each stimulus orientation. Size and velocity of stimulus bar were 1·2 × 0·4 deg and 4·0 deg s^{-1}, respectively. Bin width, 80 ms. The recovery PSTHs were obtained 2–6 min after stopping the BMI administration. Other conventions, as in Fig. 2. *B*, orientation tuning curves of responses shown in *A*.

IVa, IVb and VI were 19·9, 15·9, 16·4 and 16·4 deg, respectively. A major difference among control responses was the directionality, that is, the difference in response size between stimulus orientation at the optimal and 180 deg. This difference was particularly obvious in layer IVb and less clear in the other layers. Responses to the other stimulus orientations were also facilitated during the BMI administration (dotted line) and the orientation tuning became broader than that of the control in layers II/III (interblob) and IVb (Fig. 8*A* and *B*), but not in layers IVa and VI (*C* and *D*). However, the clear bias toward the optimally oriented stimulus remained even during the blockade of cortical inhibition in all the layers. The half-widths at half-height of the tuning peak during the BMI administration for layers II/III, IVa, IVb and VI were 30·9, 16·4, 24·6 and 15·2 deg, respectively (Fig. 8). The effect of BMI on the half-width of the orientation tuning curve was clearest in the layer II/III and absent in layer VI. The facilitatory effect on responses to the non-preferred orientation (optimal ± 60, ± 90 and ± 120 deg) was evident in layers II/III, IVa and IVb, but not in layer VI. These results suggest that in layers II/III (interblob), IVa, and IVb, the excitatory inputs to orientation-selective cells broadly tune with a bias to the optimal orientation, and that inhibitory inputs have a function in sharpening the orientation tuning, while in layer VI the orientation tuning of the response is dependent almost exclusively on that of the excitatory inputs.

To further elucidate input mechanisms of orientation selectivity, we produced averaged tuning curves to estimate relative contribution of excitatory and inhibitory inputs to the responses of the twenty-six orientation-selective (control OSI ⩾ 0·50) cells shown in Fig. 8 (Fig. 9). In this figure, the curve of excitation (continuous line) represents an averaged tuning curve during the BMI administration shown in Fig. 8 (dotted line), and the tuning curve of inhibition (Fig. 9, dotted line) represents an average of the difference in magnitude of responses obtained during the BMI administration and in the control, which were normalized to the optimal response during the BMI administration. For this calculation, we assumed that the control response of a cell reflects the simple summation of excitatory and inhibitory input. We also consider that inhibitory input has an indirect component corresponding to the inhibition of neighbouring cells that excite the cell under study. This indirect inhibition was reduced by an unknown amount

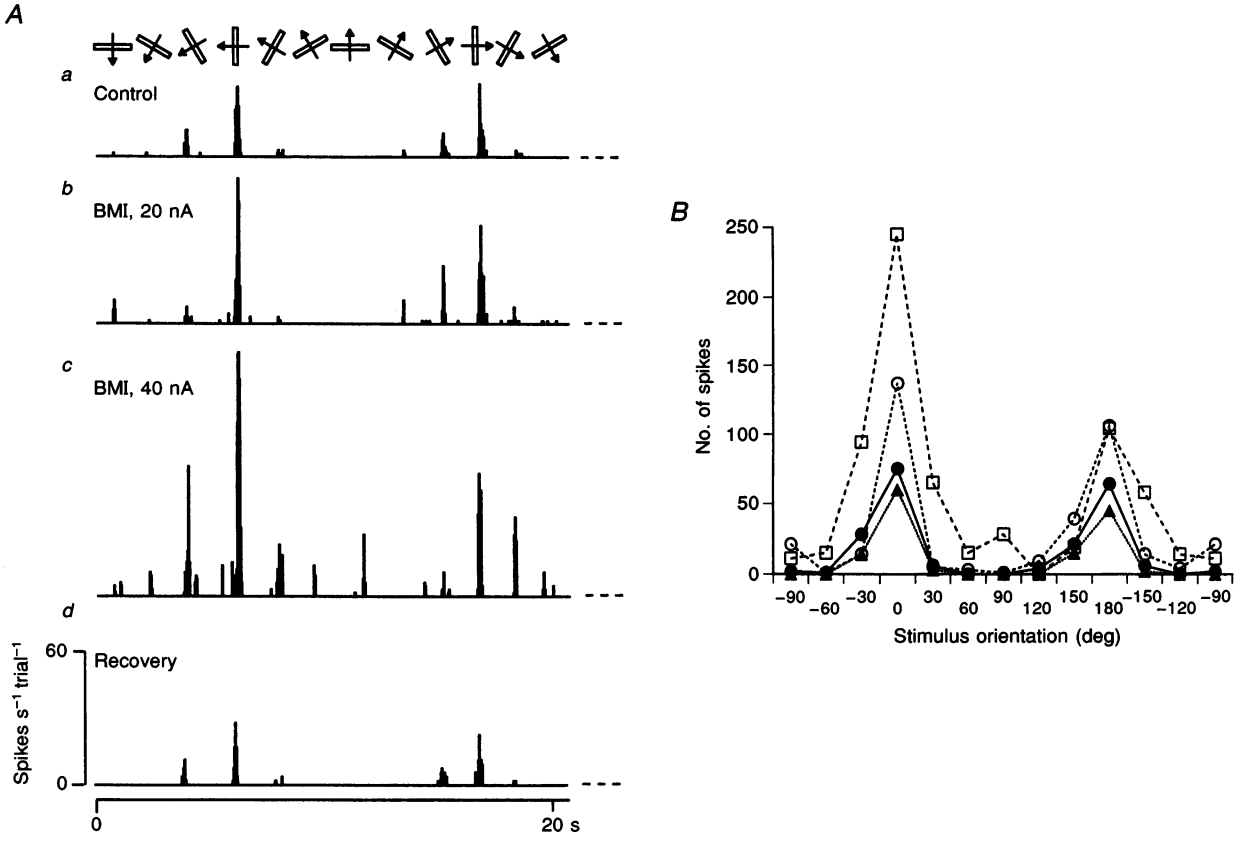

Figure 7. An example of the effect of BMI on visual responses of a layer VI cell

A, PSTHs before (*a*), during 20 nA (*b*) or 40 nA (*c*) of BMI administration and recovery (*d*). Eight sweeps for each stimulus orientation. Size and velocity of stimulus bar were 0·8 × 0·2 deg and 4·0 deg s^{-1}, respectively. Bin width, 80 ms. The recovery PSTHs were obtained 4–7 min after stopping the BMI administration. Other conventions, as in Fig. 2. *B*, Orientation tuning curves of responses shown in *A*. ●, control; ○, BMI, 20 nA; □, BMI, 40 nA; and ▲, recovery.

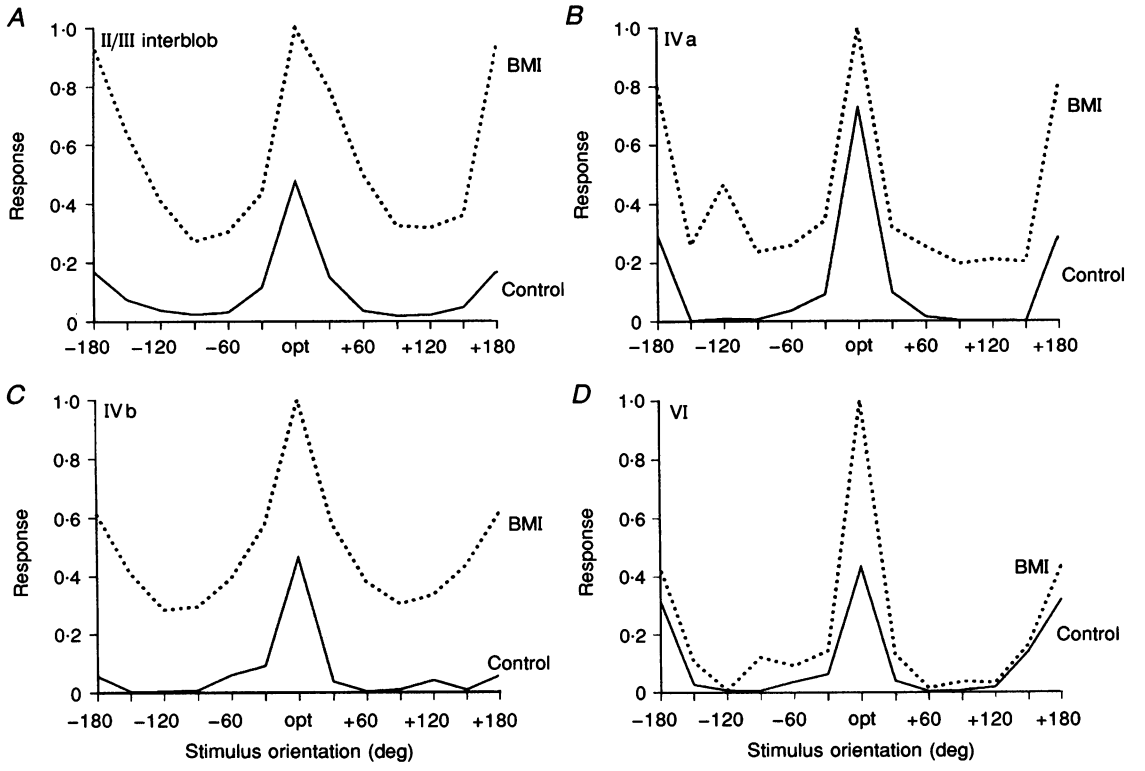

Figure 8. Averaged tuning curves of visual response of orientation-selective cells (OSI ⩾ 0·50) in each layer

Each tuning curve of visual responses was obtained by averaging control responses and responses during the BMI administration, which were normalized to the optimal response during the BMI administration of each cell. In all graphs, stimulus orientation (abscissae) indicates deviated angle of stimulus orientation from the optimal (opt). Continuous line, the control trials; dotted line, the BMI trials. *A*, layer II/III, $n = 15$; *B*, layer IVa, $n = 3$; *C*, layer IVb, $n = 5$; *D*, layer VI, $n = 3$.

during the BMI administration. Thus, the tuning curves shown in Fig. 9 roughly indicate orientation tuning of a net excitation and inhibition fed to the recorded cell in the local cortical circuit. These tuning curves take the maximal values at the optimal orientation and the minimal at the orientation orthogonal to the optimal. In contrast to the sharp peak of excitation at the optimal orientation, however, inhibitory inputs had a less prominent peak around the optimal orientation. This suggests that the proportion of the magnitude of excitatory inputs to that of inhibitory inputs at the optimal orientation is larger than that at the other orientations. In other words, contribution of inhibition to the response is less pronounced or that of excitation is more amplified near the optimal orientation than non-optimal orientations. This kind of relationship between the excitation and inhibition should have a functional implication for sharpening orientation selectivity of cells in the sense that the inhibition suppresses responses to the non-optimally oriented stimuli strongly while sparing responses to the optimal stimulus.

Test of spike saturation

In this study, it is important to ascertain that the change of orientation selectivity of cells during the BMI administration

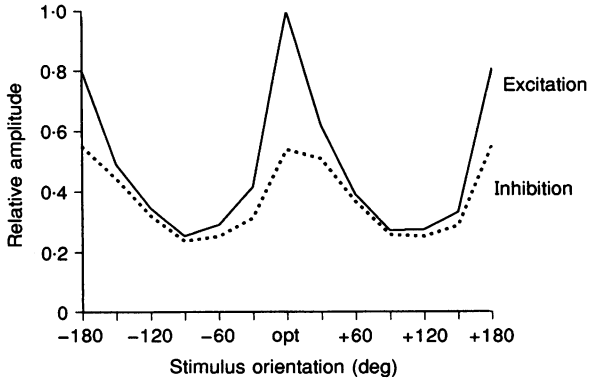

Figure 9. Averaged tuning profiles of excitation and inhibition for orientation-selective cells in monkey V1

The values were calculated from data of strongly orientation-selective cells ($n = 26$) in layers II/III (interblobs), IVa, IVb and VI shown in Fig. 8. Continuous and dotted lines indicate orientation tuning of excitation and inhibition onto the orientation-selective cell, respectively.

is not due to spike saturation in the optimal response. As one of the tests for this, we compared the orientation tuning of responses with different levels of excitatory inputs under blockade of cortical inhibition in seven cells. First we recorded the control responses to the stimulus at the usual brightness contrast (19·5 and 1·4 cd m^{-2} for the stimulus bar and background, respectively), then the effect of BMI on the orientation tuning was tested with ejecting current between +8 and +30 nA, which induced a similar range of facilitation of responses as in the previous series of experiments. Then, the brightness of the stimulus bar was reduced to the value which evoked the same response as that in the control trial without BMI. If spike saturation in the optimal response is responsible for the reduction of the orientation selectivity, the tuning curve of responses to the low-contrast stimulus should have a steeper peak around the

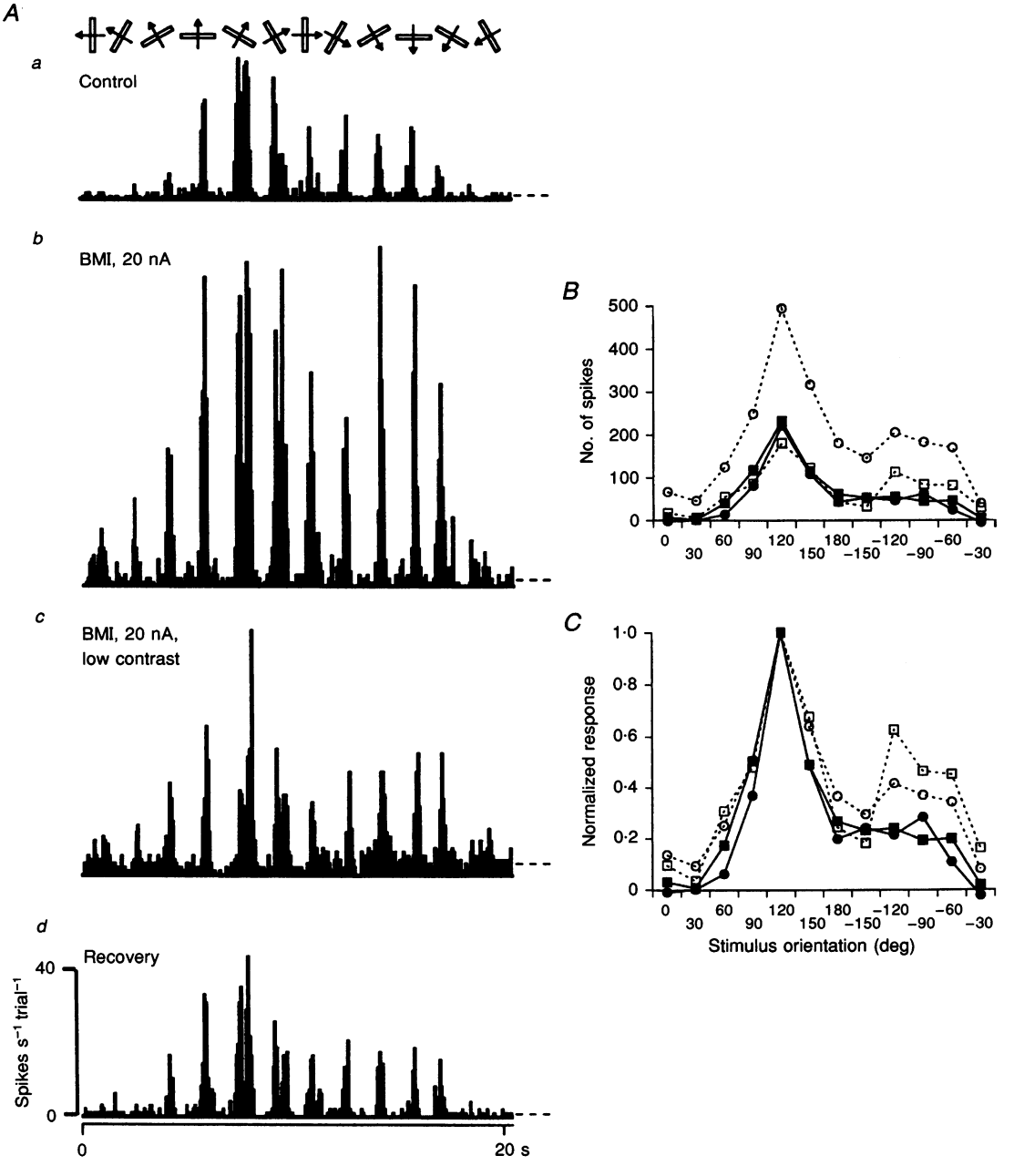

Figure 10. An example of spike saturation test in a layer IVb cell

A, PSTHs before (*a*), during 20 nA of BMI administration (*b* and *c*) and recovery (*d*). Brightness of the stimulus bar, 19·5 cd m^{-2} for *a*, *b* and *d*, and 2·0 cd m^{-2} for *c*, against the background brightness of 1·4 cd m^{-2}. Twelve sweeps for each stimulus orientation. Size and velocity of stimulus bar were 2·0 × 0·4 deg and 4·0 deg s^{-1}, respectively. Bin width, 80 ms. The recovery PSTHs were obtained 3–7 min after stopping the BMI administration. Other conventions, as in Fig. 2. *B*, orientation tuning curves of responses shown in *A*. *C*, orientation tuning curves normalized to the optimal response. ●, control; ○, BMI, 20 nA; □, BMI, 20 nA (low contrast); and ■, recovery.

optimal response than that of the BMI trials with the usual (high-contrast) stimulus, since the cell would have more room to increase its response to the saturation level in the low-contrast stimulus condition. An example of this test is shown in Fig. 10. This cell was located in layer IVb and had directional responses (Fig. 10*A a*) with OSI 0·42 to the usual stimulus. During BMI administration, responses to virtually all stimulus orientations were facilitated and the OSI was reduced to 0·27 (Fig. 10*A b*). Then, the brightness of the stimulus bar was lowered to 2·0 cd m^{-2}, to make the optimal response comparable to that at the control (Fig. 10*A c*) and the OSI of these responses was 0·34. As shown in the tuning curves in Fig. 10*B* and *C*, response tuning around the optimal orientation did not vary between the two contrast conditions. This suggests that spike saturation did not occur at the level of disinhibition used in this cell.

Averaged orientation tuning curves of responses of all the seven cells during the control, the BMI administration and the BMI administration with low-contrast stimulus are shown in Fig. 11. In this figure, each curve was normalized to the optimal response. The orientation tuning during BMI administration with a low-contrast stimulus showed a slightly broader, rather than steeper, peak around the optimal orientation compared with that during the BMI administration with a normal-contrast stimulus. This result again suggests that our protocol of BMI administration did not induce spike saturation in the optimal response.

DISCUSSION

Orientation selectivity of each layer

The laminar difference of orientation selectivity of V1 neurones observed in this study is similar to that reported previously (Livingstone & Hubel, 1984), i.e. the orientation tuning of V1 neurones is generally broad in layer IVc and blobs in layer II/III, and sharp in layers IVa, IVb and VI and interblobs in layer II/III (Figs 1, 4 and 5). Layers IVcα and IVcβ are input layers of V1 and receive their main inputs from magnocellular and parvocellular layers of the dorsal lateral geniculate nucleus (LGN), respectively (Lund, Henry, MacQueen & Harvey, 1979; Blasdel & Lund, 1983; Fitzpatrick, Lund & Blasdel, 1985). Even though the main population of cells in both of these layers did not exhibit strong orientation selectivity, layer IVcα cells had more oriented responses than IVcβ cells (Figs 1 and 5). Regarding the monkey LGN, there seem to be no studies which have systematically analysed orientation sensitivity of magnocellular and parvocellular neurones. Therefore, it is not clear whether the difference in orientation selectivity we observed between IVcα and IVcβ is due to difference in geniculate inputs or intracortical mechanisms.

In spite of a small number of samples ($n = 3$), all of the layer IVa cells showed very sharp orientation tuning (Fig. 1). This seems inconsistent with the previous observation that cells in layer IVa had orientation-insensitive response properties (Blasdel & Fitzpatrick, 1984). All of the three cells were monocularly driven as reported by Blasdel & Fitzpatrick, and two cells were colour insensitive. Since layer IVa is the thinnest layer of V1, it was hard to collect enough cells to draw a conclusion on this point. However, there might be a population of orientation-selective cells concomitant with non-oriented cells in layer IVa.

Cells in layer IVb had well-oriented responses. This layer is known to receive inputs from layer IVcα (Fitzpatrick *et al.* 1985; Lund, 1988). Iontophoretically administered BMI significantly decreased the averaged OSI of this layer to 0·24, which is comparable to 0·27 calculated from source cells in layer IVcα. These results suggest the following two points. First, inhibitory mechanisms operate in the elaboration of orientation selectivity in layer IVb. Second, since the orientation selectivity remained to a lesser extent in most of the cells during the blockade of the cortical inhibition, orientationally biased excitatory inputs to layer IVb cells exist.

In layer II/III, blob cells and interblob cells seem to be two different populations of cells with respect to orientation selectivity (Figs 1 and 4). It is to be noted that the removal of the intracortical inhibition facilitated firing activities of blob cells (Fig. 3, for example). This suggests that the inhibitory system certainly operates in blobs even though the effect of BMI on the orientation tuning of blob cells was obscure because of poor selectivity of them in the control. Blobs receive both magnocellular and parvocellular inputs

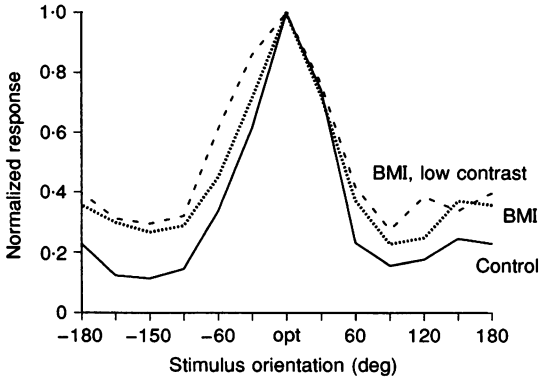

Figure 11. Averaged orientation tuning curves of spike saturation test

Orientation tuning curves of the 7 cells tested were averaged and normalized. Continuous line, control; dotted line, BMI; dashed line, BMI (low contrast).

from layers IVcα and IVcβ, and also from the geniculate interlaminar zone (Lachica, Beck & Casagrande, 1992; Hendry & Yoshioka, 1994). This system is supposed to participate in colour information processing (Livingstone & Hubel, 1984). We recently reported that the intracortical inhibition operates so as to make blob cells selective to a particular colour (Sato *et al.* 1994).

Cells in the interblob region of layer II/III showed orientation tuning much sharper than that of blob cells (Figs 1–4). Interblob cells are known to receive inputs mainly from layer IVcβ (Livingstone & Hubel, 1984; Lachica *et al.* 1992) and are supposed to deal with form vision (Livingstone & Hubel, 1988). A blockade of intracortical inhibition significantly reduced orientation selectivity (Figs 1 and 4) and the orientation tuning curves during the BMI administration revealed broad tuning of excitatory inputs (Figs 2 and 8*A*). The intracortical inhibition which also tuned broadly around the optimal orientation seems to contribute to sharpening the orientation tuning of interblob cells in layer II/III.

Layer VI cells were also well oriented on average. This layer is known to receive inputs from layers II/III, IVcα, IVcβ and V and also directly from both parvocellular and magnocellular geniculate afferents (Lund *et al.* 1979; Fitzpatrick *et al.* 1985). Because the effect of the BMI administration on the averaged OSI is small (see Figs 1, 5*D* and 8*D*), the orientation tuning of this layer seems to be more dependent on well-oriented excitatory inputs, presumably inputs from interblob regions of layer II/III.

Input mechanisms

The blockade of intracortical GABAergic inhibition by iontophoretic administration of BMI facilitated firing activity of cells in all of the layers from II/III to VI of V1 and decreased their orientation selectivity to a varying extent. This implies that the intracortical inhibition operates to a varying degree in practically all V1 cells.

In the analysis of averaged tuning curves of excitation and inhibition of orientation-selective cells (Fig. 9), both tuning curves took the maximal values at the optimal orientation and the minimal at the orientation orthogonal to the optimal. However, inhibitory inputs had a less prominent peak around the optimal orientation compared with the sharp peak of excitatory ones. This result suggests that the ratio of inhibition to excitation at slightly different orientations from the optimal is larger than that at the optimal orientation. Consequently, a dominance of excitatory inputs over inhibitory inputs is accentuated just at the optimal orientation so that the orientation tuning is sharpened around the optimal orientation.

Our results are partly consistent with previous intracellular (Ferster, 1986; Douglas *et al.* 1991; Sato *et al.* 1991) and extracellular (Sillito, 1975; Tsumoto *et al.* 1979) recording studies on the mechanisms of the orientation selectivity. Tuning curves shown in Fig. 9 look similar to the model of input mechanisms underlying orientation selectivity proposed by Ferster (Fig. 14B of Ferster, 1986), in which both excitatory and inhibitory inputs are tuned to the optimal orientation. However, there is a marked difference between our model and Ferster's; our model contains both excitatory and inhibitory inputs at orientations orthogonal and near-orthogonal to the optimal (Fig. 9). Such inputs may explain the results of previous extracellular recording studies with iontophoresis of bicuculline: orientation-selective cells became responsive to the stimulus oriented orthogonal to the optimum during the blockade of the intracortical inhibition in the cat area 17 (Sillito, 1975; Tsumoto *et al.* 1979). Bonds (1989) also suggested that, assuming the presence of orientation-biased excitation, weak tonic suppression truncates the spontaneous discharge as well as the weaker responses to non-optimally oriented stimuli and, consequently, only the stronger excitation from optimally oriented stimuli can make the cell fire. The appearance of responses to the non-optimal stimulus during BMI administration suggests that synapses which transmit broadly tuned excitation to the orientation-selective cells exist on them and the inhibitory mechanism makes them orientation-selective by suppressing responses to non-optimally oriented stimuli. Thus, it is likely that the orientation tuning of excitatory and inhibitory inputs to V1 cells is broader than that observed in extracellularly recorded responses at the control level and that the degree of orientation selectivity is controlled by the interaction of excitatory and inhibitory inputs: both have peaks around the optimal orientation.

Sources of lateral inhibitory inputs

The orientation tuning of both the excitatory and inhibitory inputs to most cortical neurones has a peak around the optimal orientation (Fig. 9). This suggests that inputs from the home or neighbouring orientation columns may have the strongest influence on the activity of the cells. However, the averaged tuning analysis (Figs 8 and 9) also suggests that there are inhibitory inputs at any stimulus orientation. This might be due to the inputs from non-oriented cells in the home column, but might also be due to interactions between columns with different orientation preferences. We previously reported that, using cross-correlation analysis in the cat area 17, the inhibitory interaction of cells was most often observed in cell pairs with slightly different (23–45 deg) orientation preferences, suggesting a contribution of inhibitory inputs originating from other orientation columns to sharpening the orientation selectivity (Hata *et al.* 1988; Hata, Tsumoto, Sato & Tamura, 1991). In the cross-correlation analysis, it is often difficult to distinguish inhibition from excitation if the dominant excitatory connection is mixed with the inhibitory one. This was probably the case at the optimal orientation in the cross-correlation study: at orientations slightly different from the optimal the relative strength of excitatory to inhibitory inputs is reduced so that the inhibitory connection became more easily detectable with the cross-

correlation analysis. This interpretation is consistent with the present results that the tuning curve of inhibitory inputs within the range of ±30 deg to the optimal orientation showed a much smaller peak than that of excitatory inputs (Fig. 9).

Technical limitations

There are at least four technical limitations for the BMI iontophoresis method. First, if the blockade of the cortical inhibition induced too strong a depolarization of cells, then the excitatory response should be saturated. This might be particularly problematic in the responses to the stimuli inducing strong excitation, i.e. the optimal and near-optimal stimuli. If this were the case, the analysis of input mechanisms (Figs 8 and 9) might underestimate the contribution of excitatory inputs to the optimal response. However, in our test of spike saturation (Figs 10 and 11), there was no sign of the spike saturation in the optimal response in the presence of a level of BMI that induced a similar level of firing facilitation to that of most other cells tested. Therefore, response saturation is not the main reason for the observed changes in orientation selectivity by BMI administration.

Second, there is a possibility that the iontophoretically administered BMI facilitated activity of not only the recorded cell but also the adjacent cells in the same and other orientation columns. If this were the case, a removal of intracortical inhibition could cause a facilitation of lateral excitatory inputs which lead to the facilitation of broadly tuned responses. Although it is hard to estimate exactly the extent of a diffusion of BMI, Fox, Sato & Daw (1989) estimated the effective diffusion area of the excitatory amino acid antagonist D-2-amino-5-phosphonovaleric acid (APV) as 100–200 μm from the tip of the electrode. This estimate should be applicable to the present experiments because they used a similar range of ejecting currents, and there are no uptake mechanisms for either BMI or APV. Considering the smaller tip diameter of our electrodes (2–4 μm) compared with theirs (7–10 μm) and that we adjusted the ejecting currents so as not to elicit strong facilitation of spontaneous activity, the diffusion area would be less than 200 μm.

Third, there is a possibility that the iontophoretically administered BMI did not block all of the inhibitory synapses of recorded cells. Since the major targets of inhibitory synapses to visual cortical neurones are their cell bodies, proximal dendritic shafts and initial segments (Somogyi, 1989), the iontophoretically administered BMI in the present study should effectively antagonize the major population of $GABA_A$ receptors on the cell under observation.

Finally, since BMI is a selective antagonist of $GABA_A$ receptors, we could not assess a possible role of $GABA_B$ receptors in orientation selectivity. In the visual cortex of the cat, however, a preliminary study reported that an iontophoretic administration of an effective antagonist for $GABA_B$ receptors to cortical neurones did not alter their orientation and direction selectivities (Baumfalk & Albus, 1988). Thus, the role of $GABA_B$ receptors in orientation selectivity may be negligible if the results in cats are applicable to the monkey V1.

Batschelet, E. (1965). *Statistical Methods for the Analysis of Problems in Animal Orientation and Certain Biological Rhythms.* American Institute of Biological Science, Washington, DC.

Baumfalk, U. & Albus, K. (1988). Phaclofen antagonizes baclofen-induced suppression of visually evoked responses in the cat's striate cortex. *Brain Research* **463**, 398–402.

Bishop, P. O., Coombs, C. S. & Henry, G. H. (1973). Receptive fields of simple cells in the cat striate cortex. *Journal of Physiology* **231**, 31–60.

Blakemore, C. & Tobin, E. A. (1972). Lateral inhibition between orientation detectors in the cat's visual cortex. *Experimental Brain Research* **15**, 439–440.

Blasdel, G. G. & Fitzpatrick, D. (1984). Physiological organization of layer 4 in macaque striate cortex. *Journal of Neuroscience* **4**, 880–895.

Blasdel, G. G. & Lund, J. S. (1983). Termination of afferent axons in macaque striate cortex. *Journal of Neuroscience* **3**, 1389–1413.

Bonds, A. B. (1989). Role of inhibition in the specification of orientation selectivity of cells in the cat striate cortex. *Visual Neuroscience* **2**, 41–55.

Chapman, B., Zahs, K. R. & Stryker, M. P. (1991). Relation of cortical cell orientation selectivity to alignment of receptive fields of the geniculocortical afferents that arborize within a single orientation column in ferret visual cortex. *Journal of Neuroscience* **11**, 1347–1358.

Douglas, R. J., Martin, K. A. C. & Whitteridge, D. (1988). Selective responses of visual cortical cells do not depend on shunting inhibition. *Nature* **332**, 642–644.

Douglas, R. J., Martin, K. A. C. & Whitteridge, D. (1991). An intracellular analysis of the visual responses of neurones in cat visual cortex. *Journal of Physiology* **440**, 659–696.

Ferster, D. (1986). Orientation selectivity of synaptic potentials in neurons of cat primary visual cortex. *Journal of Neuroscience* **6**, 1284–1301.

Fitzpatrick, D., Lund, J. S. & Blasdel, G. G. (1985). Intrinsic connections of macaque striate cortex: Afferent and efferent connections of lamina 4C. *Journal of Neuroscience* **5**, 3329–3349.

Fox, K., Sato, H. & Daw, N. (1989). The location and function of NMDA receptors in cat and kitten visual cortex. *Journal of Neuroscience* **9**, 2443–2454.

Hata, Y., Tsumoto, T., Sato, H., Hagihara, K. & Tamura, H. (1988). Inhibition contributes to orientation selectivity in visual cortex of cat. *Nature* **336**, 815–817.

Hata, Y., Tsumoto, T., Sato, H. & Tamura, H. (1991). Horizontal interactions between visual cortical neurones studied by cross-correlation analysis in the cat. *Journal of Physiology* **441**, 593–614.

Heggelund, P. & Moors, J. (1983). Orientation selectivity and the spatial distribution of enhancement and suppression in receptive fields of cat striate cortex cells. *Experimental Brain Research* **52**, 235–247.

HENDRY, S. H. C. & YOSHIOKA, T. (1994). A neurochemically distinct third channel in the macaque dorsal lateral geniculate nucleus. *Science* **264**, 575–577.

HUBEL, D. H. & WIESEL, T. N. (1962). Receptive fields, binocular interaction and functional architecture in the cat's visual cortex. *Journal of Physiology* **160**, 106–154.

HUBEL, D. H. & WIESEL, T. N. (1968). Receptive fields and functional architecture of monkey striate cortex. *Journal of Physiology* **195**, 215–243.

LACHICA, E. A., BECK, P. D. & CASAGRANDE, V. A. (1992). Parallel pathways in macaque monkey striate cortex: Anatomically defined columns in layer II. *Proceedings of the National Academy of Sciences of the USA* **89**, 3566–3570.

LIVINGSTONE, M. & HUBEL, D. (1988). Segregation of form, color, movement, and depth: Anatomy, physiology, and perception. *Science* **240**, 740–749.

LIVINGSTONE, M. S. & HUBEL, D. H. (1984). Anatomy and physiology of a color system in the primate visual cortex. *Journal of Neuroscience* **4**, 309–356.

LUND, J. S. (1973). Organization of neurons in the visual cortex, area 17, of the monkey (*Macaca mulatta*). *Journal of Comparative Neurology* **147**, 455–496.

LUND, J. S. (1988). Anatomical organization of macaque monkey striate visual cortex. *Annual Review of Neuroscience* **11**, 253–288.

LUND, J. S., HENRY, G. H., MACQUEEN, C. L. & HARVEY, A. R. (1979). Anatomical organization of the primary visual cortex (area 17) of the cat. A comparison with area 17 of the macaque monkey. *Journal of Comparative Neurology* **184**, 599–618.

MERIGAN, W. H., KATZ, L. M. & MAUNSELL, J. H. R. (1991). The effects of parvocellular lateral geniculate lesions on the acuity and contrast sensitivity of macaque monkeys. *Journal of Neuroscience* **11**, 994–1001.

RAMOA, A. S., SHADLEN, M., SKOTTUN, B. C. & FREEMAN, R. D. (1986). A comparison of inhibition in orientation and spatial frequency selectivity of cat visual cortex. *Nature* **321**, 237–239.

SÁRY, G., VOGELS, R., KOVÁCS, G. & ORBAN, G. A. (1995). Responses of monkey inferior temporal neurons to luminance-, motion-, and texture-defined gratings. *Journal of Neurophysiology* **73**, 1341–1354.

SATO, H., DAW, N. W. & FOX, K. (1991). An intracellular recording study of stimulus-specific response properties in cat area 17. *Brain Research* **544**, 156–161.

SATO, H., KATSUYAMA, N., TAMURA, H., HATA, Y. & TSUMOTO, T. (1994). Broad-tuned chromatic inputs to color-selective neurons in the monkey visual cortex. *Journal of Neurophysiology* **72**, 163–168.

SATO, H., KATSUYAMA, N., TAMURA, H., HATA, Y. & TSUMOTO, T. (1995). Mechanisms underlying direction selectivity of neurons in the primary visual cortex of the macaque. *Journal of Neurophysiology* **74**, 1382–1394.

SCHILLER, P. H., LOGOTHESIS, N. K. & CHARLES, E. R. (1990). Functions of the colour-opponent and broad-band channels of the visual system. *Nature* **343**, 68–70.

SILLITO, A. M. (1975). The contribution of inhibitory mechanisms to the receptive field properties of neurones in the striate cortex of the cat. *Journal of Physiology* **250**, 305–329.

SILLITO, A. M., KEMP, J. A., MILSON, J. A. & BERARDI, N. (1980). A re-evaluation of the mechanisms underlying simple cell orientation selectivity. *Brain Research* **194**, 517–520.

SOMOGYI, P. (1989). Synaptic organization of GABAergic neurons and $GABA_A$ receptors in the lateral geniculate nucleus and visual cortex. In *Neural Mechanisms of Visual Perception*, ed. LAM, D. M.-K. & GILBERT, C. D., pp. 35–62. Gulf Publishing Co., Houston, TX, USA.

TSUMOTO, T., ECKART, W. & CREUTZFELDT, O. D. (1979). Modification of orientation sensitivity of cat visual cortex neurons by removal of GABA-mediated inhibition. *Experimental Brain Research* **34**, 351–363.

TSUMOTO, T., MASUI, H. & SATO, H. (1986). Excitatory amino acid transmitters in neuronal circuits of the cat visual cortex. *Journal of Neurophysiology* **55**, 469–483.

VOLGUSHEV, M., PEI, X., VIDYASAGAR, T. R. & CREUTZFELDT, O. D. (1993). Excitation and inhibition in orientation selectivity of cat visual cortex neurons revealed by whole-cell recordings in vivo. *Visual Neuroscience* **10**, 1151–1155.

WONG-RILEY, M. (1979). Changes in the visual system of monocularly sutured or enucleated cats demonstrable with cytochrome oxidase histochemistry. *Brain Research* **171**, 11–28.

ZEKI, S. & SHIPP, S. (1988). The functional logic of cortical connections. *Nature* **335**, 311–317.

Acknowledgements

We thank Dr Nigel W. Daw for the critical reading of the manuscript, Dr Akichika Mikami for his computer software for stimulus presentation, and Drs Fumitaka Kimura, Yumiko Yoshimura and Hiroshi Kage for discussions. This work was supported by a grant from the International Human Frontier Science Program Organization to T.T., a Grant-in-Aid for Science Research from the Japanese Ministry of Education, Science, and Culture to H.S. and T.T. and a grant from the Ichiro Kanehara Foundation to H.S.

Author's present address

H. Tamura: Department of Biosignaling, National Institute of Bioscience and Human-Technology, Agency of Industrial Science and Technology, 1-1 Higashi, Tsukuba, Ibaraki 305, Japan.

Received 12 October 1995; accepted 2 April 1996.